Reliability analysis of the PMU microwave communication networks using generalised stochastic Petri nets

Bhargav Appasani*

School of Electronics Engineering,
KIIT University,
Bhubaneswar, 751024, India
Email: appybarkas@gmail.com

Dusmanta Kumar Mohanta*

Department Electrical and Electronics Engineering,
Birla Institute of Technology,
Mesra, 835215, India
Email: dkmohanta@bitmesra.ac.in
*Corresponding author

Abstract: The phasor measurement units (PMUs) have evolved as powerful extrapolations of the supervisory control and data acquisition (SCADA) systems due to their profound application in the real time monitoring of the smart grid (SG). In the SG several such PMUs continuously generate the time tagged phasor measurements which are communicated to a central monitoring station known as the phasor data concentrator (PDC). The communication system plays a pivotal role in the transfer of the phasor measurements to the PDC and thus should be highly reliable. This article presents a detailed approach for the construction of the generalised stochastic Petri nets (GSPNs) for the reliability analysis of the synchrophasor microwave communication networks. These communication networks are optimally planned to achieve maximum reliability without compromising the system observability. Results from the case studies for the North Eastern power grid of India are presented to demonstrate the efficacy of the proposed approach.

Keywords: reliability; smart grid; phasor measurement unit; PMU; generalised stochastic Petri nets; GSPN.

Reference to this paper should be made as follows: Appasani, B. and Mohanta, D.K. (2020) 'Reliability analysis of the PMU microwave communication networks using generalised stochastic Petri nets', *Int. J. Power and Energy Conversion*, Vol. 11, No. 1, pp.99–116.

Biographical notes: Bhargav Appasani received his BE in Electronics and Communication Engineering and ME in Wireless Communication Engineering from the Birla Institute of Technology, Ranchi, India, in 2012 and 2014, respectively, where he is currently working toward his PhD degree. He is also working as an Assistant Professor at the Kalinga Institute of Industrial Technology, Bhubaneswar, India. His research interests include wide-area measurement system communication system and evolutionary computation.

Dusmanta Kumar Mohanta received his PhD in Electrical Engineering from the Jadavpur University, Kolkata, India, in 2005. He was an electrical engineer at the Captive Power Plant, National Aluminium Company, Angul, India, from 1991 to 1998. Currently, he is working as a Professor in the Department of Electrical and Electronics Engineering, Birla Institute of Technology, Mesra, India. He has more than 20 years of teaching experience in addition to his industrial experience of eight years. He is an editor for Electric Power Components and Systems (Taylor & Francis). He has been a member of the IEEE Power and Energy Society Reliability, Risk and Probability Applications subcommittee; a life member of the Indian Society for Technical Education and a fellow of the Institutions of Engineers (India). He is an Associate Editor for IEEE ACCESS as well as for IET Proceedings on Generation, Transmission and Distribution.

1 Introduction

The modern power system integrates several technologies with the aim of providing uninterrupted quality power to the consumers (Adibi and Adibi, 2006; Tesseron, 2008). It is the advanced version of the conventional power grid characterised by bidirectional flow of electricity and information between the electricity providers and the electricity consumers and is also termed as smart grid (SG) (Amin and Wollenberg, 2005; Gellings et al., 2004). A crucial component of the SG is the synchrophasor measurement system (SPMS) which is responsible for the real time monitoring and control of the grid (Bobba et al., 2012; Ree et al., 2010). The SPMS consists of three major components, namely, the phasor measurement units (PMUs), the phasor data concentrator (PDC) and their communication network (Phadke and Thorp, 2008). The PMUs are basically sensors which are installed on the electrical buses to constantly measure the voltage and current phasors (Mohanta et al., 2016). These phasors are time tagged using the global positioning system (GPS) signal and are communicated to the PDC. The PDC collects the sensor data obtained from several PMUs, aligns the data according to their time tags and analyses the data (Phadke, 2008). The PMU and the PDC constitute the computational elements of the SPMS. The data received in the PDC is analysed for decision making by an expert. The expert may be power system engineer or data analytics software attached to the PDC (Brahma et al., 2017). The backbone for this system is the synchrophasor communication network which is responsible for the flow of information from one component to another (Lloret et al., 2012). The SPMS with all the constituent components is shown in Figure 1.

The reliability analysis of the PMU has been sufficiently dealt with in the literature Wang et al. (2009), Peng and Chan (2012) and Cherukuri et al. (2015). Different techniques such as the hierarchical Markov model (HMM) (Wang et al., 2009), Monte-Carlo simulation (MCS) (Peng and Chan, 2012), systems approach (Cherukuri et al., 2015), etc. have been proposed for computing the reliability indices. Similarly, several data mining and data analytics techniques have been proposed for effective decision-making (Wang et al., 2016; Hu and Vasilakos, 2016; Rafferty et al., 2017). However, the reliability analysis of the synchrophasor communication network has not been adequately presented in the literature (Ghosh et al., 2013a, 2013b). The challenging aspect of this analysis is to construct the network, identify the constituent components

and then compute the reliability indices. This task becomes more difficult when the microwave (wireless) technology is used for the purpose of communication in the SPMS (Atef, 2016). Recently, a systematic approach for construction of microwave communication networks (MCNs) for the PMUs has been presented for risk hedging in a smart grid (Appasani and Mohanta, 2017) and for minimisation of propagation delay in WAMS (Appasani and Mohanta, 2018). These works use the reliability block diagram (RBD) approach for the reliability analysis of the communication networks. The RBD approach uses the series-parallel network approach for calculating the reliability parameters and cannot model simultaneous component failures. Also, these previous works do not attempt to enhance the availability of the communication networks. These networks are a part of critical infrastructure of a nation's power grid and so maximising their availability is essential for reliable operation of the grid. The motivation for the work is to develop a systematic approach for computing the reliability parameters using the generalised stochastic Petri nets (GSPNs) and to construct reliable MCNs for a practical SPMS of the North-Eastern power grid of India.

Figure 1 The constituent components of the SPMS (see online version for colours)

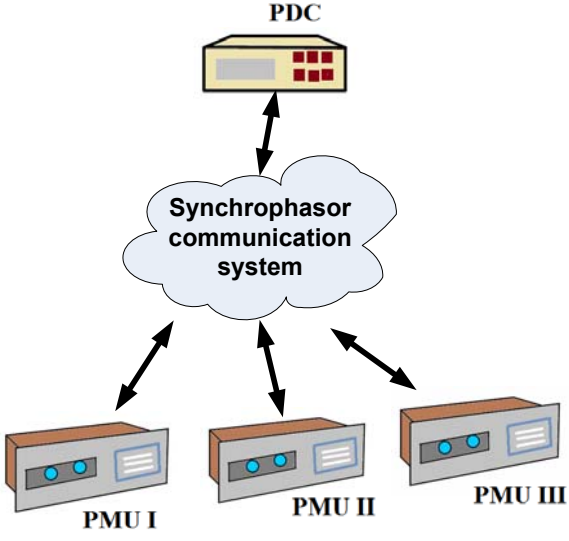

The organisation of the paper is as follows: the second section gives a comprehensive description of GSPNs. The GSPN model for a two component systems and for a single component system are also presented in this section. The third section gives a brief overview of the MCNs for the synchrophasor communication. The constituent components of the communication network and the approach for constructing these networks are presented. The GSPN models for the various subsystems of the MCN are constructed and a general approach for computing the reliability of the MCN is presented here. The fourth section presents the optimal placement algorithm for achieving maximum availability of the MCNs. Simulation results for the case study of North Eastern power grid of India are presented in the fifth section and finally the conclusions are drawn in the last section.

2 Overview of GSPNs

Petri nets (PNs) are used for modelling the behaviour of a wide range of systems that are parallel, concurrent, distributed, etc. (Murata, 1989; Kleyner and Volovoi, 2010). When stochastic time specifications are added to PNs, one obtains the GSPN (Marsan et al., 1991). A GSPN is characterised by the equation (1).

$$GSPN = \left(P, T, I, O, H, M\left(t_0\right)\right) \tag{1}$$

where $P = \{p_1, p_2, \ldots, p_k\}$ is the set of 'k' places, $T = \{t_1, t_2, \ldots, t_m\}$ is the set of 'm' transitions, $H = \{h_1, h_2, \ldots, h_l\}$ is the set of 'l' inhibitor arcs, I is the input function, O is the output function and $M(t_0)$ is the initial marking. The matrices I and O are given by equation (2). The complete description of the GSPN is presented in Marsan et al. (1991) and is beyond the scope of the paper. The GSPN is explained with the help of an example as shown in Figure 2.

Figure 2 GSPN and the reachability graph (see online version for colours)

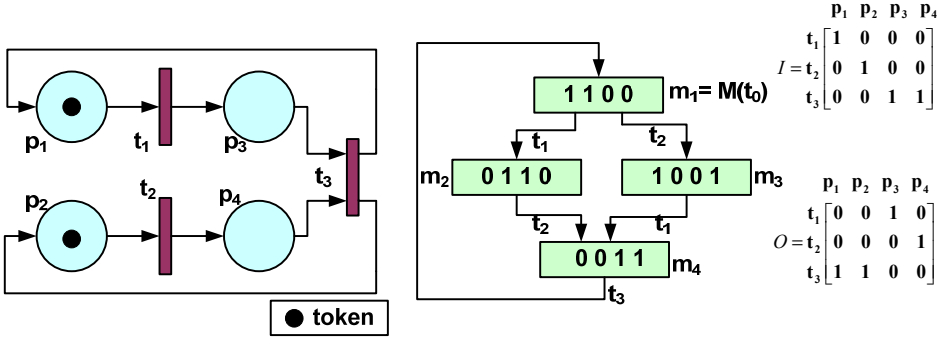

The GSPN shown in Figure 2 has $P = \{p_1, p_2, p_3, p_4\}$ and $T = \{t_1, t_2, t_3\}$. Initially, the tokens are present in places p_1 and p_2. Thus, the initial marking $m_1 = \{1, 1, 0, 0\}$. When the transition t_1 gets fired, the token in p_1 is removed and a token is added to p_3. This changes the marking to m_2. Similarly, the other markings can be obtained. The reachability graph for these markings is also shown in the Figure 2. The Markov model can be obtained from the reachability graph, which is used for computing the steady state availabilities (A_i's). The process of obtaining these parameters for the GSPN shown in Figure 2 is explained as follows:

$$\sum_{i=1}^{n} A_i = 1 \tag{2}$$

where A_i is the steady state availability of the i^{th} marking (state). For the example in Figure 2, there are four states. The state availability vector for this example is: $A = [A_1, A_2, A_3, A_4]$. This is related to the state transition matrix Q by the following relationship (Ebeling, 2004):

$$AQ = 0 \tag{3}$$

$$Q = \begin{bmatrix} -(t_1 + t_2) & t_1 & t_2 & 0 \\ 0 & -t_2 & 0 & t_2 \\ 0 & 0 & -t_1 & t_1 \\ t_3 & 0 & 0 & -t_3 \end{bmatrix} \tag{4}$$

Thus, the steady state availabilities (probabilities) can be obtained from the GSPN model of a system.

2.1 GSPN model of a two component and a single system

A two component system consists of two components operating in parallel mode. The system fails only when both the components fail. This system is shown Figure 3(a). Its GSPN model and the reachability graph is shown in Figure 3(b).

Figure 3 (a) Two component system (b) GSPN model and reachability graph (see online version for colours)

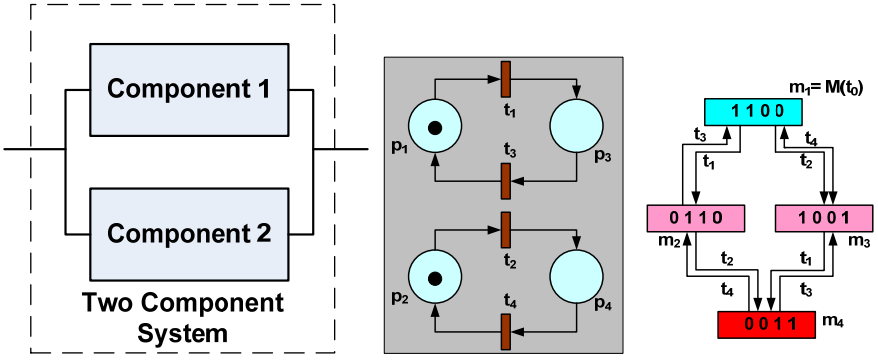

(a) (b)

In the reachability graph, the turquoise colour markings indicate fully operational states (UP state), the rose colour markings indicate semi-operational states and the red colour markings indicate failed states. From Figure 3(b) it can be understood that the markings m_1, m_2 and m_3 are operational states and the marking m_4 is a failed state. The state transition matrix for the two component system can be derived from the reachability graph and is represented in equation (5). In the reliability engineering terminology, the transitions t_1 and t_2 are called as the failure rates of component 1 and component 2 respectively. Similarly, the transitions t_3 and t_4 are called as the repair rates of component 1 and component 2 respectively.

$$Q = \begin{bmatrix} -(t_1 + t_2) & t_1 & t_2 & 0 \\ t_3 & -(t_2 + t_3) & 0 & t_2 \\ t_4 & 0 & -(t_1 + t_4) & t_1 \\ 0 & t_4 & t_3 & -(t_3 + t_4) \end{bmatrix} \tag{5}$$

The steady state probability that the system would be available is given by equation (6) and the probability that the system would be unavailable is given by equation (7). The

failure rate and the repair rate of the two component system are given by equation (8) and equation (9) respectively (Ebeling, 2004).

$$A_{UP} = A_1 + A_2 + A_3 \tag{6}$$

$$A_{DOWN} = A_4 \tag{7}$$

$$\lambda_{two\_comp} = \frac{A_{DOWN}\left(t_3 + t_4\right)}{1 - A_{DOWN}} \tag{8}$$

$$\mu_{two\_comp} = \left(t_3 + t_4\right) \tag{9}$$

A single component system is shown Figure 4(a). Its GSPN model and the reachability graph are shown in Figure 4(b).

Figure 4 (a) Single component system (b) GSPN model and reachability graph (see online version for colours)

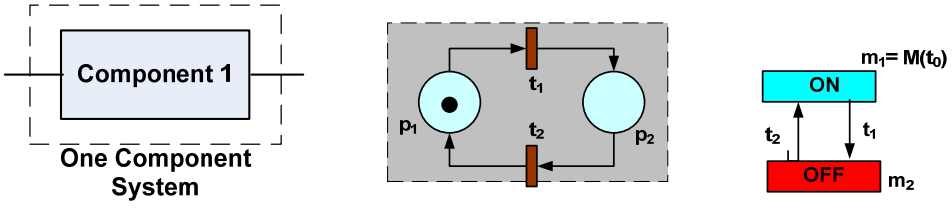

(a) (b)

The state transition matrix for the single component system can be derived from the reachability graph and is represented in equation (10).

$$Q = \begin{bmatrix} -t_1 & t_1 \\ t_2 & -t_2 \end{bmatrix} \tag{10}$$

The steady state probability that the system would be available is given by 'A_1'and the probability that the system would be unavailable is given by 'A_2'.

3 GSPN models for the synchrophasor communication networks

MCNs requires line of sight (LoS) for propagation. In the absence of LoS, repeaters are placed at regular intervals to ensure end-to-end communication. The constituent components of the MCNs for the SPMS have been comprehensively explained in the literature (Appasani and Mohanta, 2017, 2018; Freeman, 1997; Lehpamer, 2004). The main components of this system are the radio terminals, the intermediate repeaters and the antenna. The PMU generates the data which is converted into a radio frequency (RF) signal using the radio terminal. The antenna converts the RF signal into electro-magnetic signal. Intermediate repeaters are placed at regular intervals to maintain signal quality. At the PDC the signal is converted back into an electrical signal and is processed to retrieve the data. This block diagram of the system is shown in Figure 5 and it also consists of other passive components such as the connecting cables for the

antennas, the isolators, etc. which have a very low failure rate and are usually omitted from the reliability analysis. The failure rates and the repair rates of the chief constituent components of this communication network are shown in Table 1.

Figure 5 The constituents of a synchrophasor MCN (see online version for colours)

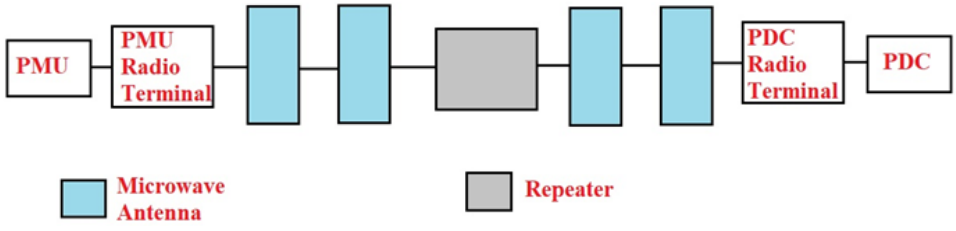

Table 1 Constituent component failure rates and repair rates

Component	*λ (failures/hr.)*	*μ (repairs/hr.)*
Single PMU radio terminal	5.7078E-06	0.2222
Single microwave repeater	1.1765E-05	0.2222
Single PDC radio terminal	5.7078E-06	0.2222
Single antenna	3.47E-07	0.0417

For enhancing the reliability, the same (1 + 1) redundancy proposed in Appasani and Mohanta (2017, 2018) has been considered. This redundancy not only enhances the system reliability but it also improves the communication link availability (Lehpamer, 2004). The various blocks present in a single repeater MCN for the SPMS along with the component redundancy is illustrated in Figure 6.

Figure 6 Redundancy SPMS MCN (see online version for colours)

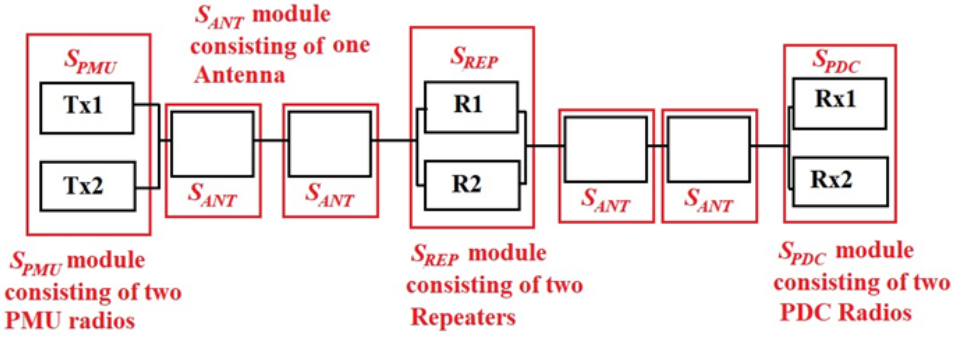

The PMU radio terminal, the PDC radio terminal and the repeater are two component systems whereas the microwave antenna is a single component system. Another observation is that the MCN with 'N' intermediate repeaters consists of the following modules: a two component PMU radio terminal module (S_{PMU}), a two component PDC radio terminal module (S_{PDC}), '2N' number of two component repeater modules (S_{REP}) and '2N + 2' antennas (S_{ANT}). The reliability analysis of this complex system is accomplished in two stages. In the first stage the steady state availabilities of the two

component modules are evaluated by constructing their GSPN models. In the next stage the two component modules are treated as single component modules with revised failure rates (obtained from the first stage) and the overall availability of the MCN is obtained by constructing the composite GSPN model.

3.1 First stage of reliability analysis

The GSPN models for the S_{PMU}, S_{PDC} and S_{REP} modules are similar to the GSPN model of the two component system shown in Figure 3(b). The interpretations of the transition $\{t_1, t_2, t_3, t_4\}$ and the places $\{p_1, p_2, p_3, p_4\}$ for these modules are shown in Table. 2. Subsequently, the state transition matrices for these modules are constructed and the steady state availabilities are computed using equations (5) to (8). These values are shown in Table. 3. Also shown in the table are the failure rates and repair rates of the two component modules.

Table 2 Interpretations for the transitions and the places for modules S_{PMU}, S_{PDC} and S_{REP}

Module	*Place*	*Interpretation*	*Transition*	*Interpretation*	*Transition value*
S_{PMU}	p_1	Tx1 is UP	t_1	Tx1 is DOWN	5.7078E-06
	p_2	Tx2 is UP	t_2	Tx2 is DOWN	5.7078E-06
	p_3	Tx1 is DOWN	t_3	Tx1 is UP	0.2222
	p_4	Tx2 is DOWN	t_4	Tx2 is UP	0.2222
S_{PDC}	p_1	Rx1 is UP	t_1	Rx1 is DOWN	5.7078E-06
	p_2	Rx2 is UP	t_2	Rx2 is DOWN	5.7078E-06
	p_3	Rx1 is DOWN	t_3	Rx1 is UP	0.2222
	p_4	Rx2 is DOWN	t_4	Rx2 is UP	0.2222
S_{REP}	p_1	R1 is UP	t_1	R1 is DOWN	1.1765E-05
	p_2	R2 is UP	t_2	R2 is DOWN	1.1765E-05
	p_3	R1 is DOWN	t_3	R1 is UP	0.2222
	p_4	R2 is DOWN	t_4	R2 is UP	0.2222

Table 3 Availability, failure rate and repair rate for modules S_{PMU}, S_{PDC}, S_{REP}

Module	A_{UP}	A_{DOWN}	λ_{two_comp}	μ_{wo_comp}
S_{PMU}	0.99999999934018	0.00000000065982	0.00000000029322	0.4444
S_{PDC}	0.99999999934018	0.00000000065982	0.00000000029322	0.4444
S_{REP}	0.9999999971968	0.0000000028032	0.0000000012457	0.4444

3.2 Second stage of reliability analysis

Having obtained the failure rate and repair rates of the S_{PMU}, S_{PDC} and S_{REP} modules, we construct the GSPN model of the MCN consisting of 'N' repeaters. This GSPN model and the reachability graph for the 'N' repeater GSPN is shown in the Figure 7.

Figure 7 GSPN model and reachability graph for an 'n' repeater MCN (see online version for colours)

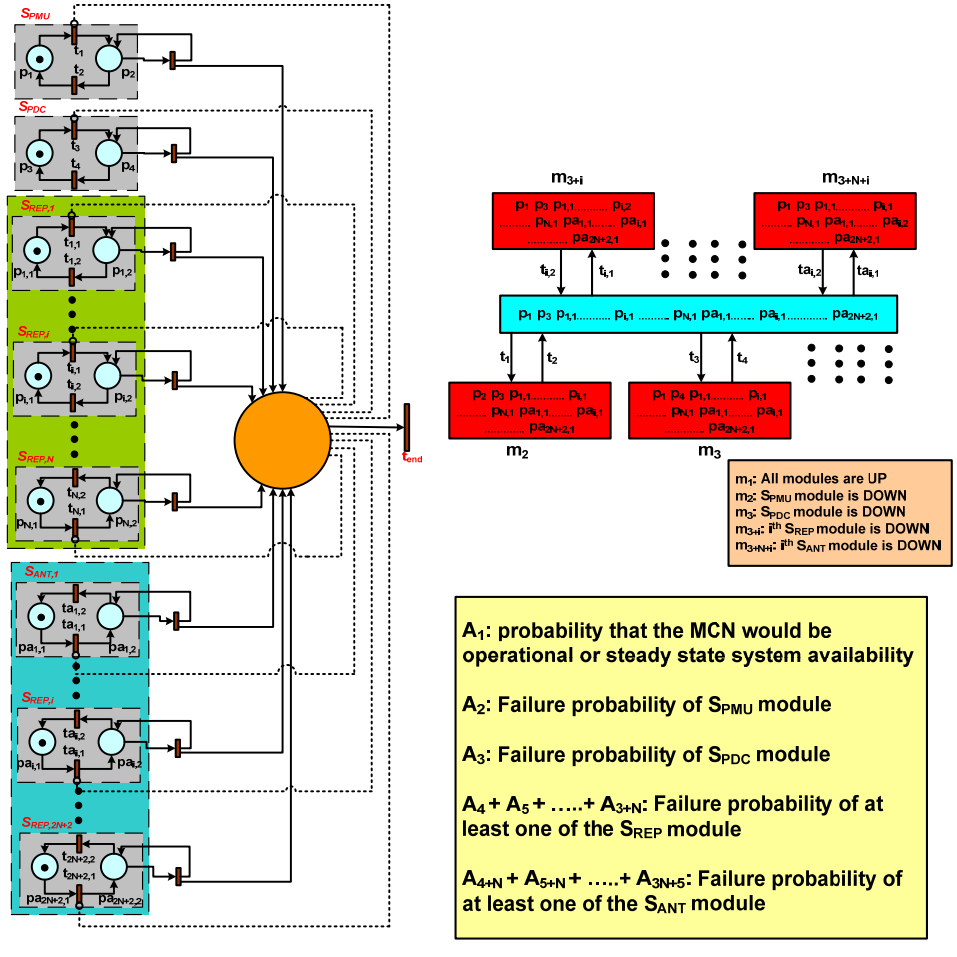

The arcs with the bubble are called as inhibitors. The transitions to which these arcs are connected can fire only when the input place does not contain any token. These arcs can be effectively employed to eliminate some of the Markov states that are highly unlikely to occur. This is a unique feature of the GSPN models which is not available in the other approaches (Ghosh et al., 2017). Transition t_{end} is not connected to any place and when it fires, tokens disappear. The interpretation of the transitions and the places are given in Table 4. The state transition matrix is given by the equation (11).

$$Q=\begin{bmatrix}
-\left(\begin{matrix}t_1+t_3\\ +\sum_{i=1}^{2N+2}ta_{i,1}+\sum_{i=1}^{N}t_{i,1}\end{matrix}\right) & t_1 & t_3 & t_{1,1} & \cdots & t_{i,1} & \cdots & t_{N,1} & \cdots & ta_{1,1} & \cdots & ta_{i,1} & \cdots & ta_{2N+1,1} & ta_{2N+2,1}\\
t_2 & -t_2 & 0 & 0 & \cdots & 0 & \cdots & 0 & \cdots & 0 & \cdots & 0 & \cdots & 0 & 0\\
t_4 & 0 & -t_4 & 0 & \cdots & 0 & \cdots & 0 & \cdots & 0 & \cdots & 0 & \cdots & 0 & 0\\
t_{1,2} & 0 & 0 & -t_{1,2} & \cdots & 0 & \cdots & 0 & \cdots & 0 & \cdots & 0 & \cdots & 0 & 0\\
\vdots & \vdots & \vdots & \vdots & \vdots & \vdots & \vdots & \vdots & \vdots & \vdots & \vdots & \vdots & \vdots & \vdots & \vdots\\
t_{i,2} & 0 & 0 & 0 & \cdots & -t_{i,2} & \cdots & 0 & \cdots & 0 & \cdots & 0 & \cdots & 0 & 0\\
\vdots & \vdots & \vdots & \vdots & \vdots & \vdots & \vdots & \vdots & \vdots & \vdots & \vdots & \vdots & \vdots & \vdots & \vdots\\
t_{N,2} & 0 & 0 & 0 & \cdots & 0 & \cdots & -t_{N,2} & \cdots & 0 & \cdots & 0 & \cdots & 0 & 0\\
\vdots & \vdots & \vdots & \vdots & \vdots & \vdots & \vdots & \vdots & \vdots & \vdots & \vdots & \vdots & \vdots & \vdots & \vdots\\
ta_{1,2} & 0 & 0 & 0 & \cdots & 0 & \cdots & 0 & \cdots & -ta_{1,2} & \cdots & 0 & \cdots & 0 & 0\\
\vdots & \vdots & \vdots & \vdots & \vdots & \vdots & \vdots & \vdots & \vdots & \vdots & \vdots & \vdots & \vdots & \vdots & \vdots\\
ta_{i,2} & 0 & 0 & 0 & \cdots & 0 & \cdots & 0 & \cdots & 0 & \cdots & -ta_{i,2} & \cdots & 0 & 0\\
\vdots & \vdots & \vdots & \vdots & \vdots & \vdots & \vdots & \vdots & \vdots & \vdots & \vdots & \vdots & \vdots & \vdots & \vdots\\
ta_{2N+1,2} & 0 & 0 & 0 & \cdots & 0 & \cdots & 0 & \cdots & 0 & \cdots & 0 & \cdots & -ta_{2N+1,2} & 0\\
ta_{2N+2,2} & 0 & 0 & 0 & \cdots & 0 & \cdots & 0 & \cdots & 0 & \cdots & 0 & \cdots & 0 & -ta_{2N+2,2}
\end{bmatrix} \tag{11}$$

Table 4 Interpretations for the transitions and the places for the 'N' repeater MCN

Place	*Interpretation*	*Transition*	*Interpretation*	*Transition value*
p_1	S_{PMU} is UP	t_1	S_{PMU} is DOWN	0.00000000029322
p_2	S_{PMU} is DOWN	t_2	S_{PMU} is UP	0.4444
p_3	S_{PDC} is UP	t_3	S_{PDC} is DOWN	0.00000000029322
p_4	S_{PDC} is DOWN	t_4	S_{PDC} is UP	0.4444
$p_{i,1}$	i^{th} S_{REP} is UP	$t_{i,1}$	i^{th} S_{REP} is DOWN	0.0000000012457
$p_{i,2}$	i^{th} S_{REP} is DOWN	$t_{i,2}$	i^{th} S_{REP} is UP	0.4444
$pa_{i,1}$	i^{th} S_{ANT} is UP	$ta_{i,1}$	i^{th} S_{ANT} is DOWN	0.000000347
$pa_{i,2}$	i^{th} S_{ANT} is DOWN	$ta_{i,2}$	i^{th} S_{ANT} is UP	0.0417

3.3 Comparison of results

Having obtained the failure rate and repair rates of the S_{PMU}, S_{PDC} and S_{REP} modules, we construct the GSPN model of the MCN consisting of 'N' repeaters. The availability of the MCNs for various values of 'N' is calculated. These results are compared with that obtained using the RBD (Appasani and Mohanta, 2017, 2018) and the comparisons are provided in Table 5.

It is observed that the availability values obtained using the proposed method is similar to those obtained using the RBD. However, using the RBD, sensitivity analysis is difficult to perform. GSPN has the ability to carry out the sensitivity analysis or the ability to identify the sensitive components of the MCN as corroborated in the fifth section.

Table 5 Comparison between RBD and GSPNs

No. of repeaters (N)	*Availability*	
	RBD (Appasani and Mohanta, 2017, 2018)	*GSPNs*
0	0.999983356	0.999983356
1	0.999966711	0.999966712
2	0.999950066	0.999950068
3	0.999933422	0.999933424
4	0.999916778	0.999916781

4 Optimal placement of PMUS

PMUs are placed in the power system in such a manner that the electrical parameters of all the buses present in the power system can be measured. This is called as observability. In order to make the entire system observable, one may be tempted to place a PMU on each and every bus in the system. But this increases the overall cost of the SPMS (More and Jadhav, 2013; Gou, 2008a, 2008b). A PMU placed on bus makes all the connected buses observable (More and Jadhav, 2013). This principle is used to place the PMUs optimally such that the system is observable with a minimum number of PMUs (More and Jadhav, 2013). Several approaches have been presented for optimally placing the PMUs and in this work the binary programming based multi-objective Genetic Algorithm (GA) has been used for optimally placing the PMUs such that the synchrophasor MCNs are maximally available. This approach is described below.

The connectivity of the electrical buses in a power system is represented using the matrix 'C' of the order ($b \times b$), whose elements are given by equation (12). Another matrix 'P' of the order ($b \times 1$) is used to indicate the locations of the PMUs in the power system. The elements of this matrix are represented using the equation (13).

$$c_{ij} = \begin{Bmatrix} 1 \text{ if } i^{th} \text{ bus is connected to } j^{th} \text{ bus or if } i = j \\ 0 \text{ else - where} \end{Bmatrix} \tag{12}$$

$$p_i = \begin{Bmatrix} 1 \text{ if the PMU is placed on the } i^{th} \text{ bus} \\ 0 \text{ else-where} \end{Bmatrix} \tag{13}$$

A multi-objective GA optimises multiple objectives simultaneously. The multi-objective GA accepts the location of the PMUs and the location of the PDC as the input and optimises two objective functions given by equations (14) and (15). The first function is a measure of the system observability and the second objective function is the measure of the availability of the MCNs between each of the PMU and the PDC.

$$f_1 = N_o + N_u + N_o N_u \tag{14}$$

where $N_o = \sum_{i=1}^{b} p_i$ is the number of PMUs

$N_u = \text{length}\left(CP < \left[1\ 1.....1\right]_{b\times 1}\right)$ is the number of buses that are unobservable using the given set of PMUs

$$f_2 = (-1)\min\left(A_{s,i}\right) \quad \forall i = 1,2,....,N_o \tag{15}$$

where $A_{s,i}$ is the availability of the MCN between the i^{th} PMU and the PDC calculated using the equation (9). The availabilities of the communication networks are to be maximised and hence a minus sign has been added before the expression in equation (13).

Algorithm 1 Repeater placement algorithm

Input: GTOPO30 DEM Data and geographical co-ordinates of the PMUs and the PDC

Output: Geographical co-ordinates of the intermediate repeaters

h = 100, D = 25000

N_o = number of PMUs

for i = 1: N_o **do**

  Node = i^{th} PMU

  LOS ← Check for existence of LOS between *Node* and PDC, j = 1, N_j = 0

  while *LOS* = 0 **do**

    d ← distance between the node and the PDC

    if $d \le D$ **and** *LOS* == 1 **do**

      break while loop

    end if

    if $d > D$ **or** *LOS* == 0 **do**

      move a distance less than D until *LOS* exists and place the j^{th} repeater of height h

      Node ← j^{th} repeater, $j = j + 1$, $N_j = N_j + 1$

      [lat_{ij}, lon_{ij}] ← Geographical co-ordinates of *Node*

      LOS ← Check for existence of LOS between *Node* and PDC

    end if

  end while

end for

In order to compute the steady state availability from equation (9), we need to know the number of repeaters that exist in the MCN. Depending on the placement of the PMUs and the PDC, the number of repeaters required for communication feasibility would vary and thus the value of the second objective function would be affected. In the practical power system, the electrical buses are separated by hundreds of kilometres and hence the topological variations of the earth's surface should be accounted for proper placement of repeaters. The topological data of the earth is available in the form of digital elevation model (DEM) data, using which the repeaters can be placed effectively (Appasani and Mohanta, 2017). This algorithm considers that the maximum distance between the intermediate towers should be less than 25 km. This constraint is necessary to maintain the link availability (Appasani and Mohanta, 2017). The intermediate tower height is

taken to be 100 m (Ghosh et al., 2013a). Without loss of generality it is assumed that if the PDC is co-located with one of the PMU's, and that there is no need of any MCN for that PMU-PDC pair. The repeater placement algorithm is given in Algorithm 1.

5 Case study: synchrophasor communication networks for North-Eastern power grid of India

The North-Eastern power grid of India consists of 14 buses and is depicted in Figure 8. The geographical co-ordinates of the electrical buses are shown in Table 6.

Table 6 Geographical co-ordinates for the North-Eastern power grid, India

Bus	*Location*	*Latitude (°N)*	*Longitude (°E)*
1	Bongaigaon	26.2626	90.2143
2	BTPS	26.4440	90.3642
3	Balipara	26.8257	92.7755
4	Khupi	24.5800	89.2560
5	B. Chariali	26.7267	93.1479
6	Ranganadi	27.3426	93.8168
7	Subansiri	27.5526	94.2588
8	Misa	26.4830	92.9330
9	Kathalguri	26.4932	92.6773
10	Mariani	26.6516	94.3283
11	Silchair	24.8333	92.7789
12	Imphal	24.8170	93.9368
13	Melriat	23.6455	92.7267
14	Pallatana	23.5097	91.4362

Source: Gopakumar et al. (2013)

Figure 8 Single line diagram of north-eastern power grid

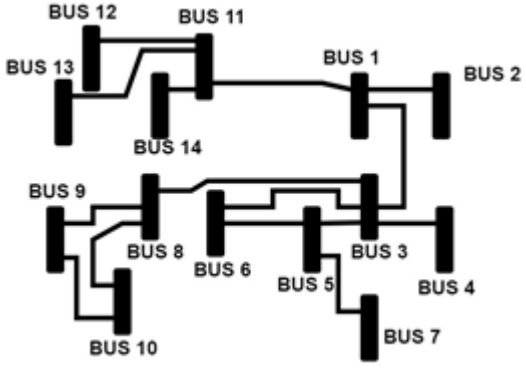

Source: Gopakumar et al. (2013)

The parameters for the multi-objective GA are taken to be: number of generations = 100; mutation rate = 0.01 and elite count = 02. The result of the optimisation process is that, with the PMUs located at bus 2 (*BTPS*), bus 3 (*Balipara*), bus 5 (*B. Chariali*), bus 9 (*Kathalguri*), bus 11 (*Silchair*) and the PDC located at bus 9 (*Kathalguri*) the MCNs for the SPMS of the North-Eastern power of India attain the maximum availability. The locations of the repeaters for the MCNs were obtained using the repeater placement algorithm and the results are shown in Table 7.

Table 7 Geographical co-ordinates of the intermediate repeaters for the North-Eastern SPMS

	MNC between PMU at Bus 2 and PDC at Bus 9 MCN-I		*MNC between PMU at Bus 3 and PDC at Bus 9 MCN-II*	
	Latitude °N	*Longitude °E*	*Latitude °N*	*Longitude °E*
PMU radio	26.4440	90.2143	26.8257	92.7755
Repeater 1	26.4510	90.6111	26.6114	92.7122
Repeater 2	26.4576	90.8581	–	–
Repeater 3	26.4638	91.1051	–	–
Repeater 4	26.4700	91.3522	–	–
Repeater 5	26.4749	91.5991	–	–
Repeater 6	26.4798	91.8462	–	–
Repeater 7	26.4843	92.0932	–	–
Repeater 8	26.4884	92.3403	–	–
Repeater 9	26.4920	92.5874	–	–
PDC radio	26.4932	92.6773	26.4932	92.6773
No. of repeaters	9		1	
	MNC between PMU at Bus 5 and PDC at Bus 9 MCN-III		*MNC between PMU at Bus 11 and PDC at Bus 9 MCN-IV*	
	Latitude °N	*Longitude °E*	*Latitude °N*	*Longitude °E*
PMU radio	26.7267	93.1479	24.8333	92.7789
Repeater 1	26.6194	92.9310	25.0576	92.7653
Repeater 2	26.5118	92.7146	25.1548	92.7594
Repeater 3	–	–	25.3268	92.7490
Repeater 4	–	–	25.5287	92.7367
Repeater 5	–	–	25.7380	92.7239
Repeater 6	–	–	25.8876	92.7147
Repeater 7	–	–	26.1119	92.7009
Repeater 8	–	–	26.3362	92.6870
Repeater 9	–	–	–	–
PDC radio	26.4932	92.6773	26.4932	92.6773
No. of repeaters	2		8	

Thus, the MCN-I requires a total of nine intermediate repeaters for communication feasibility. MCN-II requires a single repeater, MCN-III requires two intermediate repeaters and MCN-IV requires eight intermediate repeaters. The PMU co-located with

the PDC at bus 9 does not require any MCN for data transfer. These maximally available MCNs for the North-Eastern SPMS were validated for the LoS and for the link availability using the ATOLL® link planning software and are shown in Figure 9. The steady state availability and the failure probabilities of the constituent modules for each of the MCN's obtained using the equation (9) are shown in Table 8.

Figure 9 MCN's for the north-eastern SPMS (see online version for colours)

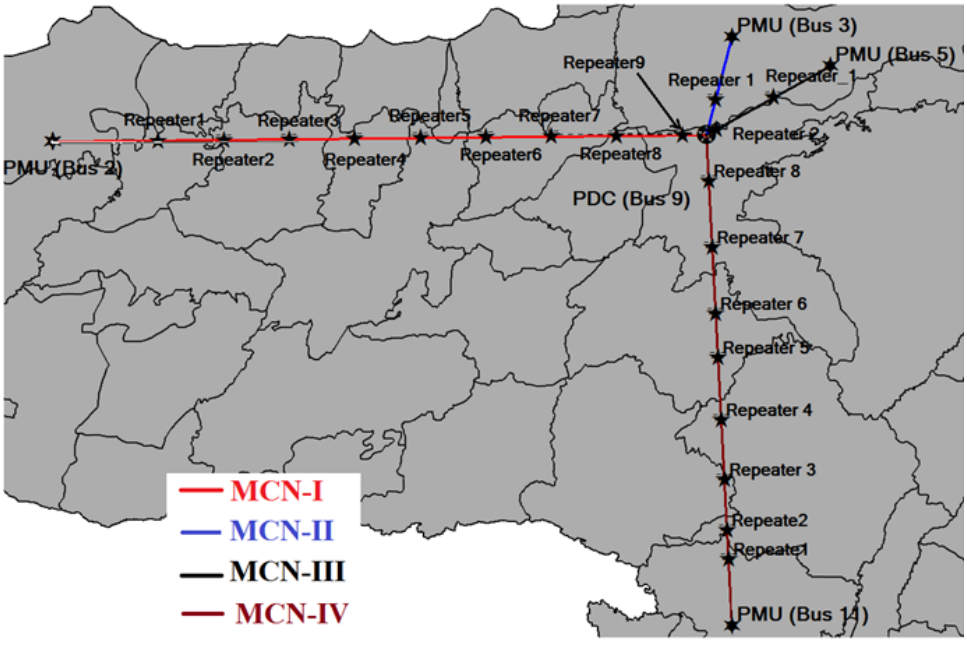

Table 8 Availability of the MCN and failure probabilities for modules S_{PMU}, S_{PDC}, S_{REP} and S_{ANT}

MCN	*Availability* (A_{MCN})	*Failure probability of the* S_{PMU} *module* (F_{PMU})	*Failure probability of the* S_{PDC} *module* (F_{PDC})
MCN-I	0.99983357429604	6.597011715911E-10	6.597011715911E-10
MCN-II	0.99996671161372	6.597890170553E-10	6.597890170553E-10
MCN-III	0.99995006750999	6.597780350929E-10	6.597780350929E-10
MCN-IV	0.99985021452192	6.597121509949E-10	6.597121509949E-10

MCN	*Failure probability of at least one of the* S_{REP} *modules* (F_{REP})	*Failure probability of at least one of the* S_{ANT} *modules* (F_{ANT})
MCN-I	2.5223749215808E-08	1.663991608061E-04
MCN-II	2.8030119996787E-09	3.328426368632E-05
MCN-III	5.6059306890063E-09	4.992556452172E-05
MCN-IV	2.2421483568496E-08	1.497617371679E-04

5.1 Sensitivity analysis

It can be observed from the Table 8 that the MCN-I between the PMU at bus 2 and the PDC at bus 9 has the minimum availability. It can also be inferred that the antenna module (S_{ANT}) has the highest probability of failure due to the lack of redundancy. Hence, by adopting a (1 + 1) redundancy for the antenna module the availability of the MCNs can be enhanced further. The availability parameters with and without the antenna redundancy are shown in Table 9.

Table 9 Availability of the MCN with and without antenna redundancy

MCN	*Availability*	
	Without redundancy	*With redundancy*
MCN-I	0.99983357429604	0.999999972067559
MCN-II	0.99996671161372	0.999999995600298
MCN-III	0.99995006750999	0.999999992658706
MCN-IV	0.99985021452192	0.999999975009151

It can be inferred from the Table 9 that by using a redundant antenna, the reliability of the MCNs can be enhanced. However, installation of redundant antennas increases the overall cost of the system.

6 Conclusions

The reliability analysis of microwave based synchrophasor communication system corroborates its efficacy for implementation even in difficult terrain having hills, forests, etc. due to its easy deployment. The component redundancy for the proposed system is also cost effective. Thus, microwave based synchrophasor communication networks seem to be a promising solution for pragmatic implementation in the power grids so as to provide maximum availability for reliable operation of the critical infrastructure.

References

Adibi, M.M. and Fink, L.H. (2006) 'Overcoming restoration challenges associated with major power system disturbances – restoration from cascading failures', *IEEE Power and Energy Magazine*, Vol. 4, No. 5, pp.68–77.

Amin, S.M. and Wollenberg, B.F. (2005) 'Toward a smart grid: power delivery for the 21st century', *IEEE Power and Energy Magazine*, Vol. 3, No. 5, pp.34–41.

Appasani, B. and Mohanta, D.K. (2017) 'Optimal placement of synchrophasor sensors for risk hedging in a smart grid', *IEEE Sensors Journal*, Vol. 17, No. 23, pp.7857–7865.

Appasani, B. and Mohanta, D.K. (2018) 'Co-optimal placement of PMUs and their communication infrastructure for minimization of propagation delay in WAMS', *IEEE Transactions on Industrial Informatics*, Vol. 14, No. 5, pp.2120–2132.

Atef, A. (2016) 'A wireless communication architecture for smart grid distribution networks', *IEEE Systems Journal*, Vol. 10, No. 1, pp.251–261.

Bobba, R.B., Dagle, J., Heine, E., Khurana, H., Sanders, W.H., Sauer, P., Yardley, T. and Phadke, A.G. (2012) 'Enhancing grid measurements', *IEEE Power Energy Magazine*, Vol. 10, No. 1, pp.67–73.

Brahma, S. et al. (2017) 'Real-time identification of dynamic events in power systems using PMU data and potential applications – models, promises and challenges', *IEEE Transactions on Power Delivery*, Vol. 32, No. 1, pp.294–301.

Cherukuri, M., Roy, D.S. and Mohanta, D.K. (2015) 'Reliability evaluation of phasor measurement unit: a system of systems approach', *Electric Power Components and Systems*, Vol. 43, No. 4, pp.437–448.

Ebeling, C.E. (2004) *An Introduction to Reliability and Maintainability Engineering*, Mc-Graw Hill, New York, NY, USA.

Freeman, R.L. (1997) *Radio System Design for Telecommunication*, Wiley, Hoboken, NJ, USA.

Gellings, C.W., Samotyj, M. and Howe, B. (2004) 'The future's smart delivery system', *IEEE Power and Energy Magazine*, Vol. 2, No. 5, pp.40–48.

Ghosh, D., Ghose, T. and Mohanta, D.K. (2013a) 'Communication feasibility analysis for smart grid with Phasor measurement units', *IEEE Transactions on Industrial Informatics*, August, Vol. 9, No. 3, pp.1486–1496.

Ghosh, D., Ghose, T. and Mohanta, D.K. (2013b) 'Reliability analysis of geographic information system (GIS) aided optimal phasor measurement unit location for smart grid operation', *Proceedings of the Institution of Mechanical Engineers*, *Part O: Journal of Risk and Reliability*, Vol. 227, No. 4, pp.450–458.

Ghosh, S., Ghosh, D. and Mohanta, D.K. (2017) 'Impact assessment of reliability of phasor measurement unit on situational awareness using generalized stochastic Petri nets', *International Journal of Electrical Power and Energy Systems*, Vol. 93, pp.75–83, 2017.

Gopakumar, P., Chandra, G.S., Reddy, M.J.B. and Mohanta, D.K. (2013) 'Optimal redundant placement of PMUs in Indian power grid--northern, eastern and north-eastern regions', *Frontiers in Energy*, Vol. 7, No. 4, p.413.

Gou, B. (2008a) 'Optimal placement of PMUs by integer linear programming', *IEEE Trans. on Power Systems*, August, Vol. 283, No. 3, pp.1525–1526.

Gou, B. (2008b) 'Generalized integer linear programming formulation for optimal PMU placement', *IEEE Transactions on Power Systems*, Vol. 23, No. 3, pp.1099–1104.

Hu, J. and Vasilakos, A.V. (2016) 'Energy big data analytics and security: challenges and opportunities', *IEEE Transactions on Smart Grid*, Vol. 7, No. 5, pp.2423–2436.

Kleyner, A. and Volovoi, V. (2010) 'Application of Petri nets to reliability prediction of occupant safety systems with partial detection and repair', *Reliability Engineering and System Safety*, Vol. 95, No. 6, pp.606–613.

Lehpamer, H. (2004) *Microwave Transmission Networks: Planning, Design and Deployment*, Mc-Graw Hill, New York, NY, USA.

Lloret, J., Lorenz, P. and Jamalipour, A. (2012) 'Communication protocols and algorithms for the smart grid [Guest Editorial]', *IEEE Communications Magazine*, Vol. 50, No. 5, pp.126–127.

Marsan, M. et al. (1991) 'An introduction to generalized stochastic Petri nets', *Microelectronics Reliability*, Vol. 31, No. 4, pp.699–725.

Mohanta, D.K., Cherukuri, M. and Roy, D.S. (2016) 'A brief review of phasor measurement units as sensors for smart grid', *Electric Power Components and Systems*, Vol. 44, No. 4, pp.411–425.

More, K.K. and Jadhav, H.T. (2013) 'A literature review on optimal placement of phasor measurement units', *IEEE International Conference on Power, Energy and Control (ICPEC)*.

Murata, T. (1989) 'Petri nets: properties, analysis and applications', *Proceedings of the IEEE*, April, Vol. 77, No. 4, pp.541–580.

Peng, Z. and Chan, K.W. (2012) 'Reliability evaluation of phasor measurement unit using Monte Carlo dynamic fault tree method', *IEEE Transactions on Smart Grid*, Vol. 3, No. 3, pp.1235–1243.

Phadke, A.G. (2008) 'The wide world of wide-area measurement', *IEEE Power and Energy Magazine*, Vol. 6, No. 5, pp.52–65.

Phadke, A.G. and Thorp, J.S. (2008) 'Phasor measurement units and phasor data concentrators', *Synchronized Phasor Measurements and Its Applications*, 1st ed., Chapter 5, pp.93–105, Springer, New York.

Rafferty, M. et al. (2017) 'Real-time multiple event detection and classification using moving window PCA', *IEEE Transactions on Smart Grid*, Vol. 7, No. 5, pp.2537–2548.

Ree, J.D.L., Centeno, V., Thorp, J.S. and Phadke, A.G. (2010) 'Synchronized phasor measurement applications in power system', *IEEE Transactions on Smart Grid*, Vol. 1, No. 1, pp.20–27.

Tesseron, J.M. (2008) 'Mission: reliability', *IEEE Power and Energy Magazine*, Vol. 6, No. 1, pp.42–48.

Wang, B. et al. (2016) 'Power system transient stability assessment based on big data and the core vector machine', *IEEE Transactions on Smart Grid*, Vol. 7, No. 5, pp.2561–2570.

Wang, Y., Li, W. and Lu, J. (2009) 'Reliability analysis of phasor measurement unit using hierarchical Markov modeling', *Electric Power Components and Systems*, Vol. 37, No. 5, pp.517–532.